Available online at www.sciencedirect.com

ScienceDirect

Procedia CIRP 108 (2022) 112–117

www.elsevier.com/locate/procedia

6th CIRP Conference on Surface Integrity

Surface finishing of EBM parts by (electro-)chemical etching

Laurent Spitaels[a,*], Édouard Rivière-Lorphèvre[a], Macarena Cantero Díaz[a], Jonathan Duquesnoy[b], François Ducobu[a]

[a]*Machine Design and Production Engineering Lab, Research Institute for Science and Material Engineering, University of Mons, Place du Parc 20, Mons 7000, Belgium*

[b]*Chimiderouil S.A., Rue des Ayettes 20, Ghlin 7011, Belgium*

* Corresponding author. *E-mail address:* laurent.spitaels@umons.ac.be

Abstract

Post treatment of titanium alloy parts obtained by Electron Beam Melting (EBM) is required before assembly due to their high roughness (Ra = 25 μm). For parts with complex geometry, chemical and electro-chemical etching are two promising processes which enhance the part surface integrity thanks to their global action. These two processes were applied to Ti6Al4V parts obtained by EBM. Their surface topography, micro hardness, dimensional and geometrical accuracy were compared. For a given removed thickness of 0.150 mm, electro-chemical etching exhibited higher efficiency to improve arithmetic roughness (~39%) than chemical etching (~7%).

Keywords: Electron Beam Melting (EBM) ; Chemical etching ; Electro-chemical etching

1. Introduction

Additive Manufacturing is opening new possibilities of part design [1] since the first introduction of a commercial 3D printer in the 1980s [2]. Diverse materials can be shaped by AM processes: polymers, metals and ceramic [3]. Within the different existing metals, titanium alloys such as Ti6Al4V is widely used in various applications (*e.g.* for the biomedical and aeronautical sectors) thanks to its strength-to-weight ratio, biocompatibility and corrosion resistance [4, 5]. Among the seven AM working principles established by ISO 52900, powder bed fusion processes such as Electron Beam Melting (EBM) is feeding great hopes thanks to its higher building rates and lower residual stresses compared to Selective Laser Melting (SLM) and Direct Energy Deposition (DED) [5]. Nevertheless, the parts manufactured by EBM process exhibit higher arithmetic roughness (Ra) than SLM and DED [5, 6]. Indeed, common reported values of Ra for as-built EBM parts can be between 25 µm and 131 µm while 0.24 µm to 13.3 µm and 5 µm to 40 µm can be respectively achieved for DED and SLM [5]. Oxidation and partially melted particles adhesion on the part's surface are the main causes of the high roughness surfaces in EBM parts [5]. Post treatments (*e.g.* polishing, chemical etching, conventional machining) are then required to overcome the EBM process defects [1, 7] since they can improve surface finish and, therefore, the strain to failure [8] and fatigue resistance [5].

AM post treatments can be classified into three categories: mechanical, radiation and chemical, depending on their working principle [7]. Two well-known mechanical processes by material removal are machining and blasting [4]. However, even if they can lead to Ra below 1 µm [9], these processes cannot be applied to very complex geometries (*e.g.* lattice structures [8] or internal features as conformal cooling channels [1]). Consequently, other post treatments have to be investigated. Two chemical post processes are promising since they allow a global action on the part: chemical etching (also named chemical machining, CM) and electro-chemical etching (also named electro-chemical machining, ECM) [9].

On the one hand, chemical etching consists in immersing the part in a chemical bath composed of a mix of acids [9]. As presented by Wysocki *et al.* [10], efficient material removal rates can be achieved for additively manufactured Ti6Al4V parts by using a mix of HF and HNO_3. On the other hand, electro-

* Corresponding author

2212-8271
10.1016/j.procir.2022.03.023

chemical etching can be seen as an inverse electro-plating operation [9]. Indeed, the part (anode) is placed into a bath of electrolyte and exchanges ions with a cathode thanks to an electrical potential difference [7, 9]. Chemical etching is simpler and less expensive than electro-chemical etching [9]. However, it achieves lower volumes of removed material than electro-chemical etching [7].

This article aims to compare the performances of chemical and electro-chemical etching applied to Ti6Al4V parts manufactured by the EBM process. A dimensional and geometrical analysis is conducted as well as a surface topography evaluation. Finally, micro hardness of the parts is evaluated and compared to an as-built part.

2. Methodology

2.1. Parts manufacturing

The design of the parts is shown in Figure 1. The geometry exhibits two different cylinders named A and B with two different diameters: 14.30 mm and 20 mm respectively. The total height of the part was set at 26.2 mm. The parts were manufactured taking their Z axis for build direction. Spherical plasma atomised Ti6Al4V ELI (Extra Low Interstitial) Grade 23 powder was used as feedstock for the printing. The granulometry distribution of this powder is centred on 70 µm (D50), while minimum and maximum diameters of particles stand at 45 µm and 106 µm respectively. Layer thickness of the printing was set at 50 µm. Eight parts were selected among the 24 produced in the same batch on an ARCAM A2 EBM printer and were used in their as-built state. A distinction is made in the following sections between the parts before (as-built) and after (treated) the chemical or electro-chemical etching post treatments.

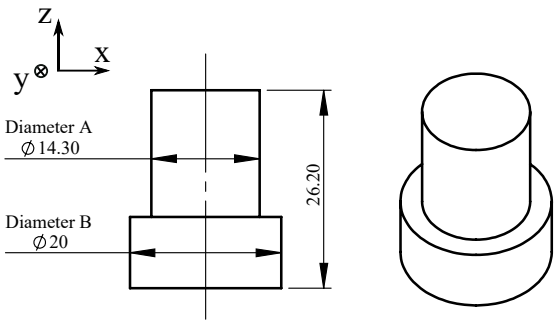

Fig. 1. Design of the parts (in mm).

2.2. Chemical etching

Six parts over the eight available were post treated using a 5-steps chemical etching. The bath was composed of HNO_3 and HF combined with water [10]. The ratio between these two acids stood at 20. Other bath parameters set by the company which treated the parts are confidential. Thickness removal was targeted to be performed in five equal steps from 50 µm up to 250 µm. After each step of 50 µm thickness removal, one part was taken from the bath to serve as an image of the step. One last part served as a witness to calibrate the bath. Each of the parts was given a name referring to the step they belong to (*e.g.* step 1, step 2, etc. and witness for the witness part).

2.3. Electro-chemical etching

One of the eight parts was electro-chemically etched using a mix of H_2SO_4 and HF for the electrolyte. Concentrations of these two chemical species are not mentioned since it is the know-how of the company which treated the parts. The electro-chemical etching configuration is given in Figure 2, while the main parameters are given in Table 1. The treated part was taken as the anode while a 38 mm inner diameter stainless steel AISI 304 tube was selected as the cathode. This geometry allowed the cathode to fit the external geometry of the treated part as much as possible. The part was centred inside the tube to keep the same spacing between the cathode and the anode. Current connection clamps were connected to the top of cylinder A while the flat surface of cylinder B (bottom of the part) remained free in order to allow the circulation of the electrolyte. According to the dimensions of the cylinders composing the part, the spacing between the cathode and cylinder B reached 9 mm, while 11.85 mm separated cylinder A from the cathode. Indeed, the space between the cathode and the anode has an influence on the electric field density on the part and, consequently, on the thickness removed [7]. A constant difference of potential of 12 V was applied between the cathode and the anode, while a constant temperature of 25°C and stirring were applied to the electrolyte. Electro-chemical treatment time was set at 20 minutes while 0.150 mm was the thickness target to remove.

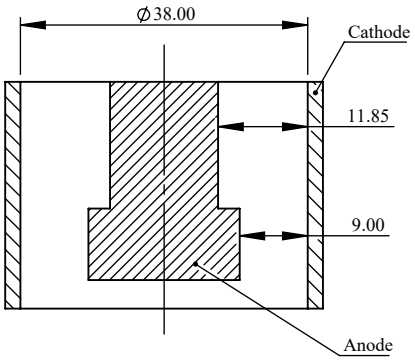

Fig. 2. Electro-chemical etching configuration (in mm).

Table 1. Electro-Chemical Etching Parameters.

Electrolyte	H_2SO_4 and HF
Cathode material	AISI 304
Difference of potential applied	12 V
Temperature	25°C
Treatment time	20 minutes
Thickness target to remove	0.150 mm

2.4. Dimensional and geometrical evaluation

The parts were evaluated in terms of dimension and geometry before and after their treatment by chemical or electro-chemical etching. These measurements were performed using a Coordinate Measuring Machine (CMM) LH54 from Wenzel at room temperature. It was equipped with a PH10M head and a 2.5 mm diameter spherical probe, both from Renishaw. The diameter of cylinders A and B were measured using eight points distributed over two circles. The total height of the parts was measured by probing six points on two planes: the top of cylinder A and the top of a steel gauge block simulating the bottom of the part. Finally, the Metrosoft QUARTIS Measurement Software version 2021 was used to compute the diameters, total length and cylindricity from the probed points. The removed thickness was evaluated by computing the half of the difference between the part diameter before and after its treatment by chemical and electro-chemical etching. All measurements were reproduced three times by rotating the parts by 120° over their Z axis.

2.5. Surface topography evaluation

Surface topography evaluation was performed using a roughness measurement instrument DH-6 from Diavite. The signal acquisition was performed using a computer while the Diasoft software version 3.1.9 computed the resulting arithmetic and total roughness (Ra and Rt respectively). All measurements presented in the following sections are an average of five measurements made on cylinder B. All measurements were taken parallel to Z axis and spaced by an angle of 72° around the parts Z axis. The evaluation length was set at 4.8 mm. Since the usual values of Ra for EBM as-built parts can be higher than 25 µm [5], it means that the measurements performed did not fulfil the ISO 4288 standard. Indeed, this standard requires an evaluation length of 40 mm to perform roughness evaluation of parts exhibiting an Ra between 10 µm and 80 µm. However, only 9.45 mm along the Z axis is available on cylinder B. The results obtained with an evaluation length of 4.8 mm should therefore be used for relative rather than absolute comparison.

2.6. Micro hardness evaluation

Micro hardness measurements were evaluated using a Vickers hardness tester machine M400-A from LECO. A force of 0.980 N was used to ensure length of indentation diagonals between 0.020 mm and 1.400 mm, as recommended by ISO 6507. The parts' cylinder A were cut at about 3 mm from cylinder B. All the samples were mounted in resin and polished using silicon carbide foils. The final polishing step was performed using a mixture of colloidal silica (OP-S) and hydrogen peroxide (30%). Images were then acquired and measured using a camera and the Image Focus software. The goal of these measurements was to emphasise the potential influence of the chemical and electro-chemical treatments on the parts micro hardness. The distance between the first indentation and the external surface of each sample was therefore set to the minimal value, as recommended by ISO 6507 (two and a half times d where d stands for the mean diagonal length of the indentation). Similarly, the distance between two indentation centres was also set to the minimal recommended value, so three times d. In total five measurements were taken from each sample surface while one measurement was also performed at its centre. Each of the measurements was repeated five times. Table 2 summarises the main parameters of the micro hardness analysis.

Table 2. Main parameters of the Vickers micro hardness evaluation.

Pyramidal indenter angle (α)	136°
Force applied	0.980 N
Force holding time	15 s
Distance between external surface and first indentation	2.5 d
Distance between consecutive indentations centres	3 d

Ti6Al4V titanium alloy exhibits α and β phases [5]. The size of the indentation should therefore be sufficient to evaluate a combination of several phases and not only one phase at a time. Figure 3 gives an image with 2000× magnification of an as-built part which has been etched with Kroll's reagent to reveal its α and β phases (this last has a brown colour). The blue losange represents the size of the smallest indentation performed during the micro hardness analysis (diagonals of 0.020 mm). All the micro indentations performed then simultaneously straddle several phases, meaning that the indentation size is sufficient to deliver reliable results of micro hardness.

Fig. 3. EBM as-built part attacked with Kroll's reagent (2000× magnification).

3. Results

3.1. Dimensional and geometrical evaluation

The resulting graphs of dimensional and geometrical analysis are given in Figure 4 and 5 with 2σ error bars.

Figure 4 depicts the average removed thickness on cylinder A and B and on the total length for the chemically etched parts (step 1 to 5), electro-chemically etched part (ECM) and the witness of the chemical etching bath (witness). As experienced previously [11], the effective thickness removed by chemical etching is lower or higher than the target for steps 1 to 5. For example, the maximum thickness removed (step 5) stands at 0.199 mm which is 0.050 mm less than the target (0.250 mm). On average, there is little difference of thickness removed between the cylinders A and B. The major difference comes from

the witness part of the chemical etching bath. Indeed, it lost 0.576 mm on average for cylinder A while cylinder B lost 0.517 mm. In the case of the electro-chemical etched part, both diameters exhibit a higher difference with an average removed thickness of 0.090 mm on the cylinder A while 0.149 mm were removed on the cylinder B. This can be explained by the difference of distance between the cylinder A and B and the cathode. The lower the gap between anode and cathode, the higher the volume of removed material [7]. In contrast, the total length reduction along the built direction of the part (Z axis) during chemical etching does not reach the same values as the thickness removed on cylinder A and B. Steps 1, 4 and 5 exhibit a lower total length reduction than the thickness reduction of cylinders A and B, while steps 2 and 3 exhibit the opposite trend. The witness part of the chemical etching faced a total length reduction of the same order of magnitude as the thickness reduction of its cylinder A. Finally, the electro-chemically etched part exhibits the same material reduction for the cylinder B and total length (0.149 mm).

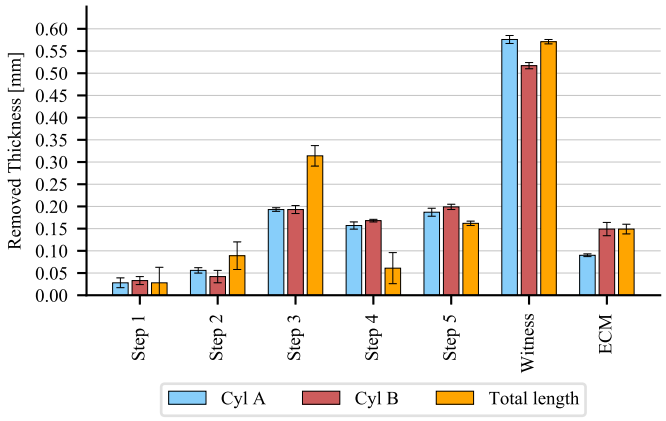

Fig. 4. Average removed thickness (in mm).

The cylinder A and B cylindricity deviations for the different chemically and electro-chemically etched parts are given in Figure 5. The mean cylindricity of the as-built cylinder A parts exhibited values between 0.070 mm and 0.133 mm (standard deviation of 0.029 mm), while the chemically etched parts from steps 1 to 5 showed more homogeneous values from 0.070 mm to 0.079 mm (standard deviation of 0.004 mm). All the parts treated by chemical etching decreased their cylindricity deviation, except for the witness part. Indeed, it exhibited the highest measured deviation for cylinder A with 0.323 mm after etching, while its as-built cylindricity deviation stood at 0.056 mm. Such a degradation after the thickness removal of 0.576 mm by chemical etching means that cylindricity deviation can be increased by the chemical etching process if too much thickness is removed. Electro-chemical etching of cylinder A decreases cylindricity deviation from 0.062 mm to 0.051 mm.

Cylinder B shows less homogeneous cylindricity deviations after chemical etching. Indeed, for steps 1 to 5, the as-built parts exhibit a cylindricity of cylinder B between 0.057 mm and 0.130 mm (standard deviation of 0.023 mm). After chemical etching, these values are between 0.052 mm and 0.092 mm (standard deviation of 0.016 mm). For almost all the parts, cylinder B benefited from a decreased cylindricity deviation thanks to the chemical etching. Only the part of step 2 showed an increase of its cylindricity deviation. However, this deviation is not significant with respect to the 2σ error bars. In the case of the electro-chemical etching, the cylinder B cylindricity deviation decreased from 0.083 mm to 0.025 mm.

A comparison can be made between the cylindricity reduction obtained after electro-chemical etching and step 3 of chemical etching. Indeed, the same thickness was removed after these two operations (about 0.150 mm). Electro-chemical etching allowed to decrease cylindricity of cylinder A and B by 18% and 70% respectively, while step 3 of the chemical etching decreased cylindricity by 14% and 44% for cylinders A and B respectively. At this stage, electro-chemical etching seems to give better results than chemical etching for the same removed thickness.

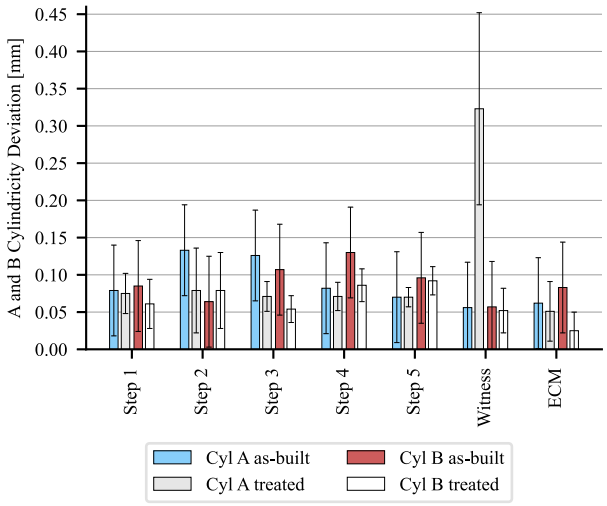

Fig. 5. Cylindricity deviation evolution for cylinders A and B (in mm).

3.2. Surface topography evaluation

The results of the surface topography evaluation is given in Figures 6, 7 and 8 with 2σ error bars. The average Ra of the as-built parts stands at 14.64 µm. As explained in section 2.5 the evaluation length does not fulfil the recommendations of ISO 4288. Therefore, the results can only be used for a relative, instead of an absolute, comparison.

Figure 6 gives the average arithmetic roughness measured on cylinder B of the different parts which endorsed the chemical and electro-chemical etching. Compared to the as-built parts, the first and second steps of the chemical etching leads to a small increase of Ra (3% and 7% respectively). However, the measurement dispersion for as-built parts is higher than the Ra reduction measured. No conclusion can therefore be drawn from this result since the reduction is not significant with respect to the measurement dispersion. Steps 3 to 5 lead to more

significant Ra reduction with respect to the as-built parts. Indeed, step 3 decreased Ra by 7%, step 4 by 11% and step 5 by 21%. As expected, the witness part benefited from the highest improvement with an arithmetic roughness decrease of 72%. The electro-chemically treated part exhibits a 39% decrease of arithmetic roughness. This last result has to be balanced with the removed thickness on cylinder B. Indeed, the electro-chemical etching allowed a 39% decrease of the arithmetic roughness while removing a 0.149 mm thickness on the part. The same thickness was removed for step 3 of the chemical etching, but it only allowed a 7% improvement of the arithmetic roughness. This shows the higher performance of the electro-chemical etching to improve arithmetic roughness while removing as little material as possible.

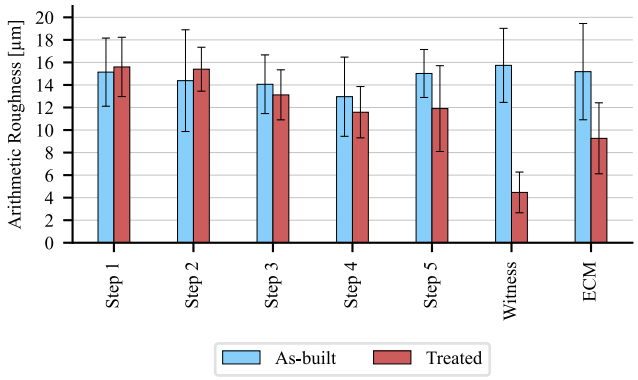

Fig. 6. Arithmetic roughness evolution for cylinder B (in µm).

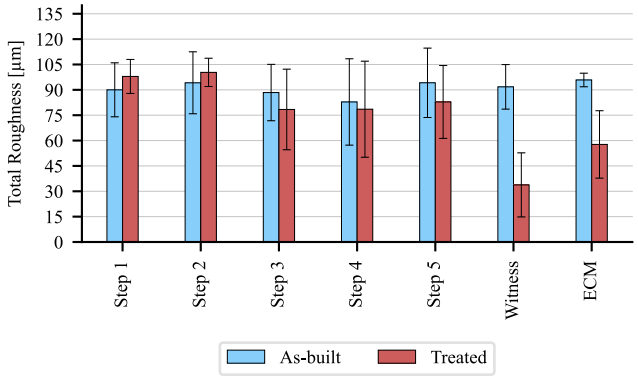

Fig. 7. Total roughness evolution for cylinder B (in µm)

The total roughness measurements of cylinder B followed the same trend as the arithmetic roughness as depicted in Figure 7. Indeed, steps 1 and 2 of the chemical etching lead to a small increase of Rt (9% and 7% respectively) while the other steps improved the total roughness by 11% for step 3, 5% for step 4 and 12% for step 5. The witness is the part facing the highest reduction of total roughness with a 63% improvement. Again, this better result has to be balanced with the removed thickness on cylinder B for this part which reaches more than 0.500 mm. The electro-chemical etching treatment allowed a 40% reduction of Rt while only removing 0.149 mm of the part diameter, so the same order of magnitude as the improvement of Ra. In opposition, it should be noted that for a given part and chemical etching step, the Rt improvement is not the same as the Ra.

As a result of the cylindrical geometry of the cathode used for electro-chemical etching, the Ra and Rt improvement for cylinder A and B are not the same as depicted in Figure 8. Indeed, the distance between cylinder A and the cathode (11.45 mm) is not the same as the distance between cylinder B and the cathode (9.0 mm). As explained by Hung [7], the volume of removed material is inversely proportional to the interelectrode gap. Accordingly, the Ra improvement for cylinder B (39%) is higher than for cylinder A (17%), while, similarly, the Rt improvement for cylinder B (40%) is higher than for cylinder A (16%). However, it should be noted that Ra and Rt are reduced for each cylinder in the same order of magnitude. Chemical etching led to less homogeneous results since Ra and Rt improvement did not reach the same value depending on the cylinder treated.

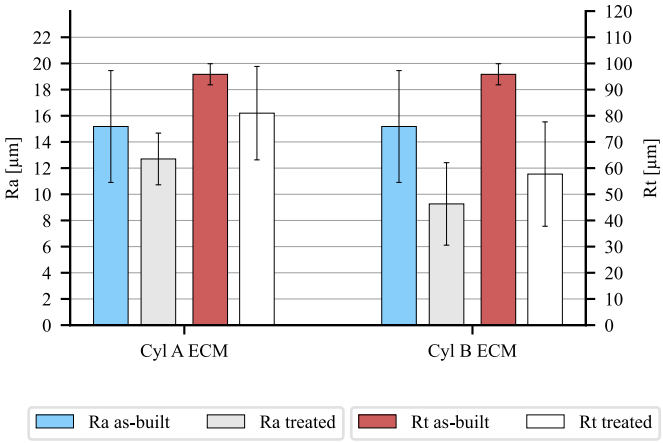

Fig. 8. Arithmetic and total roughness of electro-chemically treated part (in µm).

3.3. Micro hardness evaluation

Figure 9 gives the micro hardness measurements on cylinder A of the chemically and electro-chemically etched parts as well as one as-built part. The horizontal axis gives the radial coordinate of the indentation performed on the parts with respect to the as-built part. For example, the part of the chemical etching Step 1 lost a thickness of 0.028 mm on average. The radial coordinate of the first indentation made on this part at 0.050 mm from the external surface will then equal 0.078 mm (0.028 mm + 0.050 mm). Cylinder A of the as-built part was tested along three different radial directions spaced by 120° while taking the same radial coordinates for the indentations. Values varying from 358 HV0.1 to 407 HV0.1 were measured with an average standard deviation reaching 13 HV0.1. The micro hardness inside a part then varies depending on the region

tested. As a result, no error bars are displayed in Figure 9 to ease its analysis.

All the micro hardness measured was between 341 HV0.1 and 443 HV0.1. For each radial coordinate, high variations of micro hardness were measured. For example, step 2 of the chemical etching led to 422 HV0.1 at a radial coordinate of 0.22 mm while step 1 reached 380 HV0.1. This is consistent with the results obtained by Chern *et al.* [12] who measured values of Vickers micro hardness varying by about 5% for EBM parts in a plane perpendicular to the build direction. However, a general tendency can be seen from the graph while comparing the chemical etching steps to the as-built part. Indeed, steps 1 to 3 exhibited values of micro hardness below and above the as-built part. However, steps 4 and 5 were both above the as-built part in terms of micro hardness. This tends to show that chemical etching can slightly increase the micro hardness of the parts. Since no mechanical stress is directly induced by chemical etching, the increase is assumed to come from stresses redistribution in the part due to material removal. This tendency is less obvious for the ECM which led to values of micro hardness below and then above the as-built part, like in steps 1 to 3 of the chemical etching.

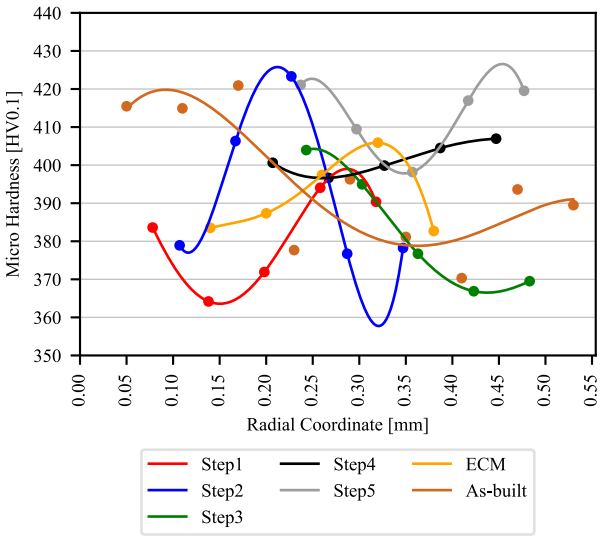

Fig. 9. Micro hardness of cylinder A (in HV0.1).

4. Conclusion

The main conclusions of this study are:

- For the same removed part thickness (0.150 mm), electro-chemical etching allows a higher reduction of cylindricity (70%) compared to chemical etching (44%).
- Depending on the parts' geometry treated, chemical etching seems to increase cylindricity deviation if too much material is removed (more than 0.5 mm).
- Electro-chemical etching allows a higher arithmetic and total roughness improvement (39% and 40% respectively) for a given thickness removed (0.150 mm) than chemical etching (7% and 11% respectively).
- The relative Ra and Rt reductions achieved are more homogeneous in the case of the electro-chemical etching than for the chemical etching.
- Chemical etching seems to slightly increase the micro hardness of the treated parts after a thickness reduction of about 0.150 mm.

References

[1] Rosen, D., Kim, S., 2020. Design and Manufacturing Implications of Additive Manufacturing, in "*Additive Manufacturing Processes*". In: Bourell, D., Frazier, W., Kuhn, H., Seifi, M. (Eds.). ASM International, 24, pp. 19–29.

[2] Bourell, D., Beaman, J., Wohlers, T., 2020. History and Evolution of Additive Manufacturing, in "*Additive Manufacturing Processes*". In: Bourell, D., Frazier, W., Kuhn, H., Seifi, M. (Eds.). ASM International, 24, pp. 11–18.

[3] Bourell, D., Kruth, J.P., Leu, M., Levy, G., Rosen, D., Beese, A., Clare, A., 2017. Materials for Additive Manufacturing. CIRP Annals 66.2, 659–681.

[4] Bagehorn, S., Mertens, T., Greitemeier, D., Carton, L., Schoberth, A., 2015, "Surface finishing of additive manufactured Ti-6Al-4V - a comparison of electrochemical and mechanical treatments," 6th European Conference for Aerospace Sciences. Krakow, Poland, paper #99.

[5] Liu, S., Shin, Y.C., 2019. Additive Manufacturing of Ti6Al4V Alloy: A Review. Materials & Design 164, article #107552.

[6] Zhao, L., Santos Macías, J. G., Dolimont, A., Simar, A., Rivière-Lorphèvre, E., 2020. Comparison of residual stresses obtained by the crack compliance method for parts produced by different metal additive manufacturing techniques and after friction stir processing. Additive Manufacturing 36, article #101499.

[7] Hung, W., 2020. Post-Processing of Additively Manufactured Metal Parts, in "*Additive Manufacturing Processes*". In: Bourell, D., Frazier, W., Kuhn, H., Seifi, M. (Eds.). ASM International, 24, pp. 298–315.

[8] de Formanoir, C., Suard, M., Dendievel, R., Martin, G., Godet, S., 2016. Improving the mechanical efficiency of electron beam melted titanium lattice structures by chemical etching. Additive Manufacturing 11, 71–76.

[9] Kalpakjian, S., Schmid, S.R., 2013. Advanced Machining Processes and Equipment, in "*Manufacturing Engineering and Technology 7th Edition*". In: Yap, E. (Ed.). Pearson Education South Asia Pte Ltd, Jurong, pp. 769–796.

[10] Wysocki, B., Idaszek, J., Buhagiar, J., Szlazak, K., Brynk, T., Kurzydlowski, K.J., Swieszkowski, W., 2019. The influence of chemical polishing of titanium scaffolds on their mechanical strength and in-vitro cell response. Materials Science and Engineering: C 95, 428–439.

[11] Spitaels, L., Ducobu, F., Demarbaix, A., Rivière-Lorphèvre, E., Dehombreux, P., 2020. Influence of Conventional Machining on Chemical Finishing of Ti6Al4V Electron Beam Melting Parts. Procedia Manufacturing 47, 1036–1042.

[12] Chern, A.H. and Nandwana, P. and Mc Daniels, R., Dehoff, R., Liaw, P., Tryon, R., Duty, C., 2020. Build orientation, surface roughness, and scan path influence on the microstructure, mechanical properties, and flexural fatigue behavior of Ti–6Al–4V fabricated by electron beam melting. Materials Science and Engineering: A 772, article #138740.